Multichannel Wireless-Electrodeless Quartz-Crystal Microbalance Immunosensor

Hirotsugu Ogi,[*,†,¶] Hironao Nagai,[†] Yuji Fukunishi,[†] Taiji Yanagida,[†] Masahiko Hirao,[†] and Masayoshi Nishiyama[‡]

Graduate School of Engineering Science, Osaka University, Machikaneyama 1-3, Toyonaka, Osaka 560-8531, Japan, and Central Workshop, Osaka University, Machikaneyama 1-2, Toyonaka, Osaka 560-0043, Japan

E-mail: ogi@me.es.osaka-u.ac.jp

Abstract

We develop the wireless-electrodeless multichannel quartz-crystal microbalance (QCM) biosensor using quartz plates of slightly different thicknesses. Their shear vibrations are simultaneously excited and detected by a pair of antenna wires to perform the noncontacting measurement. Their fundamental resonance frequencies are between 43 and 55 MHz, and vibrations at up to 10 channels are measured in liquids. Owing to high affinity of naked quartz surfaces for proteins, we immobilized various receptor proteins on different quartz plates nonspecifically and detected various antigen-antibody reactions separately. The exponential coefficient of the frequency change, rather than the amount of the frequency decrease, is found to be useful for distinguishing between specific and nonspecific binding reactions.

[*]To whom correspondence should be addressed
[†]Graduate School of Engineering Science
[‡]Central Workshop, Osaka University, Machikaneyama 1-2, Toyonaka, Osaka 560-0043, Japan
[¶]PRESTO, JST. 4-1-8 Honcho, Kawaguchi, Saitama, Japan

Introduction

Quartz-crystal microbalance (QCM) biosensor has been an important tool for studying interactions between proteins,[1–3] proteins and DNAs,[4–6] and proteins and cells.[7–9] It allows label-free monitoring of association and dissociation reactions in liquids in real time, yielding the affinity between interacting proteins.[2,10,11] The label-free detection of proteins will contribute to the diagnosis for detecting biomarkers.[12–14]

One of the central issues in the QCM study is development of the multichannel QCM (MQCM) biosensor. It will significantly increase the efficiency of detection of target proteins and enable monitoring of interactions among three or more biomolecules. It involves many other potential as described by Tatsuma *et al.*[15] and Dickert *et al.*[16] Therefore, intensive efforts have been paid for establishing MQCM biosensors. The principal approach is developing the one-chip MQCM, where several sensing regions are prepared on a single quartz plate. This MQCM is capable of monitoring the biological reactions in the same liquid environment. Besides, using one channel as a reference, it allows compensation for temperature and viscosity effects. Tatsuma *et al.*[15] made four sensor regions by chemically etching the quartz plate and confirmed their independent operation by dropping a water droplet. Abe *et al.*[17–19] succeeded in making different-thickness sensing regions in a single quartz plate by the deep-reactive ion etching method. The individual responses were measured referring different resonance frequencies: They demonstrated a four-channel measurement as a gas sensor.[17] Jin *et al.*[20] also developed a four-channel one-chip MQCM and adopted it to a gas sensor: They minimized the interference among the channels (or cross talks) by depositing the electrodes with both symmetric and asymmetric configurations. Thus, the one-chip MQCM has demonstrated high potential for increasing the channel number. However, because of the ineluctable interference among channels, no study succeeded in establishing the MQCM for an immunosensor. Another approach is the combination of many single-channel QCMs.[21] This can operate as a MQCM and the interference is negligible. However, it requires a larger amount of solutions, and the liquid environment (temperature, pressure, and so on) will be not the same among sensor cells, downplaying the important advantage of the MQCM. Also, it is not easy to

increase the number of the channel. (Many instruments are needed for individual channels.)

We here propose a wireless-electrodeless MQCM (WE-MQCM) to solve the problems in previous MQCMs. The shear vibrations of AT-cut quartz crystal plates with different thicknesses are simultaneously excited and detected by the same line antenna in the same reaction cell. Because of the independent sensor chips, the frequency interference among chips is negligible, while the reactions can be monitored in nearly the same environment. The electrodeless blank quartz plates are set in a line along the flow channel. The thickness of the quartz plates are between 39 and 30 μm, corresponding to 43 and 55 MHz fundamental resonance frequencies, respectively. Up to ten-channel WE-MQCM is developed here. (Further increase of the channel number is easily achieved using smaller crystals.) We use the nonspecific binding for immobilizing the receptor proteins, which allows the replacement-free MQCM.

The WE-MQCM is first applied to the immunosensor. We detect different immunoglobulin G (IgG); human IgG (hIgG), mouse IgG (mIgG), and rabbit IgG (rIgG) and discuss the usability of our WE-MQCM.

Experimental Section

We have developed high frequency QCMs using the spiral-coil antenna[22] and line antennas.[23,24] There are two important advantages in this wireless-electrodeless QCM. First, it is free from the deterioration of the mass sensitivity by the heavy electrodes on the quartz surfaces.[3] Second, it can immobilize receptor proteins nonspecifically without using any linkers such as a self-assembled monolayer, owing to the high affinity of proteins for the piezoelectric quartz.[25] As the result, its mass sensitivity can be improved significantly compared with conventional QCMs as demonstrated in reference 3.

In this study, we extended this method for the MQCM and developed electronics and software for monitoring resonance frequencies of many channels. We made blank AT-cut quartz plates with thicknesses between 30 and 39 μm by 1 μm step. Their diameter is 3 mm. Their both

surfaces were mechanically polished to obtain the surface roughness with R_a <0.5 nm. The quartz crystals were set in the handmade sensor cell by lightly sandwiching their edge parts by 1-mm-thick silicon gaskets (Fig. 1) after immobilization of receptor proteins. The two line-antenna wires for generation and detections of vibrations are located outside the flow channel so as to measure the resonance frequencies of all the sensor chips contactlessly.

We apply the rf burst voltage ($\sim$2 μs duration) to the generation antenna wire, located outside the flow channel, to cause the quasistatic electric field in the thickness direction of the quartz plates and then to generate the shear vibrations. After the excitation, the quartz crystals oscillate with their fundamental resonance frequencies. The detection antenna wire receives their vibrational signals through the piezoelectric effect simultaneously, which are mixed with reference sinusoidal signals using multipliers and the amplitudes and phases of the individual quartz crystals are extracted by integrating the mixed beating signals with an analog time gate using the superheterodyne method.[26,27] By sweeping the frequency of the reference signal, we can observe the amplitude spectrum as shown in Fig. 2, including a train of resonance peaks with uniform frequency spacing. The Lorentzian-function fitting provides the resonance frequency of each crystal. We repeat this frequency-scan measurement during the flow of the carrier solution. After they became stable enough (frequency fluctuation $< 10^{-7}$), we monitored phases at the individual resonances to determine the resonance-frequency changes in real time using the linear relationship between the frequency and the phase near the resonances.[28] A single measurement for acquiring the frequency changes of all channels takes about 20 ms, and we made 200-times averaging for the stable measurement and obtained them every $\sim$4 s. The standard relative deviation of the frequency fluctuation during the flow of the carrier solution is about 5×10^{-7} for 1 h.

During the flow of the solution, the temperature around the sensor cell is maintained at 37 °C in the temperature controlled box. The phosphate-buffer solution (PBS) with ph 7.4 is used as the carrier solution. We use a large flow rate (500 μL/min) for activating the binding reactions on the crystals.[24] The length, width, and height of the flow channel are 40, 3, and 2 mm, respectively.

We first confirm the operation of the individual channels using the specific binding reaction

between hIgG and staphylococuss aureus protein A (SPA) using three channels. We prepared three quartz plates, where Au ultrathin films (18 nm Au on 2 nm Cr) were deposited on both surfaces. The crystals were cleaned in a piranha solution (98%H_2SO_4:33%H_2O_2=7:3) for 1 h, and after rinsing with ultrapure water, they were immersed in a 10 mM 10-carboxy-1-pentanethiol solution for 24 h. Their surfaces were activated using a 100 mM 1-ethyl-3-(3-dimethyl aminopropyl) carbodiimide (EDC) solution for 1 h. Then, one crystal was immersed in a 10 mg/mL bovine serum albumin (BSA)/PBS for 24 h, which is used as the reference channel. The other crystals were immersed in different-concentration SPA/PBS (4 and 400 μg/mL) for 15 h at 4 °C in order to change the amount of SPA molecules immobilized on the quartz surfaces. After rinsing with the PBS, they were immersed in the 10 mg/mL BSA/PBS for 1 h as the blocking procedure. These three sensor chips are set in the sensor cell, and we inject a 515 nM hIgG solution.

Next, we adopted the five-channel WE-MQCM for detecting different antigen-antibody reactions. We prepare five quartz channels, where anti-hIgG antibody (AhIgG), anti-mIgG angibody (AmIgG), anti-rIgG antibody (ArIgG), SPA, and BSA were immobilized nonspecifically as follows: The five blank sensor chips were first cleaned in the piranha solution for 1 h and rinsed by the ultrapure water. Four of them were then immersed in the individual receptor-protein solutions (400 μg/mL antibodies/PBS and 400 μg/mL SPA/PBS) for 15 h at 4 °C. After rinsing with the PBS, they were immersed in a 10 mg/mL BSA/PBS for 1 h for blocking uncovered surfaces. The fifth sensor chip was immersed in the 10 mg/mL BSA/PBS for 24 h as the reference channel. (We have shown that antibodies, SPA, and BSA significantly adsorb on the naked quartz surfaces.[25]) Schematics of their surfaces are shown in Fig. 3.

hIgG was purchased from Athens Research and Technology (product no. 16-16-090707), and AhIgG was from Arista Biologicals Inc. (product no. ABIGG-0500). mIgG and rIgG were from Invitrogen Corporation (product no. 02-6502 and 02-6102, respectively), and AmIgG and ArIgG were from Arista Biologicals Inc. (product no. ABGAM-0500 and ABGAR-0500, respectively). SPA was from Zymed Laboratories, Inc. (product no. 10-1100). BSA was from Sigma-Aldrich Japan (product no. 9048-46-8).

Results

Figure 4 shows the result of the three-channel measurement. Broken lines show binding curves between SPA and hIgG as well as between BSA and hIgG caused by the injection of the 515 nM hIgG solution. The fundamental resonance frequencies were near 55, 53, and 52 MHz for the chips immersed in BSA, higher-concentration SPA, and lower-concentration SPA solutions, respectively. The slight mass-sensitivity differences due to the difference of the fundamental resonance frequency were corrected for the 55 MHz channel, simply by multiplying the ratio of the fundamental resonance frequencies. The largest frequency decrease is observed for the crystal immersed in the higher concentration SPA solution, indicating that the larger number of SPA molecules were immobilized. The frequency decrease is observed even for the reference channel, indicating the nonspecific binding reaction between BSA and hIgG due to the high concentration hIgG solution. The solid lines in the figure are corrected frequency changes, where the reference response was subtracted. (The reference-channel response therefore remains unchanged after the correction.)

Figures 5 (a)-(c) show the frequency changes observed in the five channel WE-MQCM measurements responding to injections of hIgG, mIgG, and rIgG solutions, respectively. (The fundamental-frequency differences were again corrected for the 55 MHz channel.) Figures 5(d)-(f) are frequency changes, where the frequency response of the BSA reference channel was subtracted. The antigen-antibody reactions are separately observed by the WE-MQCM.

Discussion

Figure 4 demonstrates that our WE-MQCM successfully operates as the multichannel immunosensor. It is well known that hIgG and SPA binds specifically each other,[29–31] and immersion of the surface activated sensor chip in the higher-concentration SPA solution should adsorb larger number of hIgG molecules, yielding a larger frequency change. The frequency changes more rapidly just after the binding reaction, which is associated with the steric hindrance effect.[24] (The apparent affinity is affected by the surrounding analyte molecules when the concentration of the analyte

is higher.) However, the overall frequency-change rate appears to be independent of the number of the immobilized receptor. This is confirmed by the thermodynamic theory in the case of a flow-injection system. The resonance frequency decreases exponentially with the exponential coefficient α given by[2,11]

$$\alpha = k_a C_A + k_d. \tag{1}$$

Here, C_A denotes the concentration of the analyte in the solution, and k_a and k_d are the association-rate and dissociation-rate constants of the binding reaction, respectively. Thus, α depends only on the protein pair and the analyte concentration, and is not affected by the number of immobilized receptor protein. The α values for the high and low receptor numbers in Fig. 4 actually agreed with each other after the correction by the reference channel (α=5.6$\pm$0.9 $\times$ 10^{-3} s^{-1}), whereas their frequency changes varied by a factor of 2 at 3000 s.

Figure 5 more clearly demonstrates the successful operation of our WE-MQCM as the immunosensor. The channel with an antibody receptor shows significantly larger frequency decrease when the corresponding antigen is injected, while other channels show lower frequency changes except for the SPA channel. The SPA binds with IgG molecules significantly, and the number of IgG molecule which can bind with a single SPA is larger than one.[30] Thus, the amount of the frequency change in the SPA channel is always larger than the other channels. rIgG especially shows higher affinity with SPA,[32] resulting in the largest frequency decrease. The simultaneous measurement allows us to observe nonspecific adsorptions. For example, it is indicated from Fig. 5(c) that AhIgG binds with rIgG with relatively higher affinity.

It is also important to note that the reference channel contributes to correct the unexpected frequency change, which occasionally occurs just after the arrival of the solution in the sensor cell. Figure 5(a), for example, shows unusual frequency change after the solution arrival, and some channels showed frequency increases. These are however appropriately corrected using the BSA channel as the reference. Such a spurious frequency change could occur in the flow-injection sys-

tem due to a mechanical disturbance in switching the pump to the other vial and due to differences of the solution temperature and viscosity. Thus, we analyzed the result by subtracting the response of the reference channel from the frequency responses as shown in Figs. 5(d)-(f).

In order to distinguish the frequency change associated with the antigen-antibody reaction from nonspecific binding reactions, we again use the exponential coefficient α. It is usually difficult to control the number of the receptor protein on the quartz surfaces in the nonspecific immobilization procedure.[25] However, the α value should not be affected by the number of the receptor protein on the quartz surfaces, and it depends only on the concentration of the analyte and the thermodynamic constants of the binding reaction. Therefore, we evaluated the binding reactions of the protein pairs in Fig. 5 with the α value as shown in Fig. 6. This figure clearly indicates that the antigen-antibody reactions take the α values much larger than those of the nonspecific bindings. For example, the α value between hIgG and AhIgG (7.9×10^{-3} s^{-1}) is larger than that between hIgG and ArIgG by a factor of 5. It is also larger than that between hIgG and SPA by a factor of 2.3, despite the larger frequency change in hIgG-SPA binding. Thus, using the exponential coefficient, it will be possible to evaluate the concentration of a target protein in solutions including other nonspecifically binding proteins, although the corresponding calibration measurement are required in advance like as all other biosensors.

Conclusion

We have developed the multichannel electrodeless quartz-crystal-microbalance immunosensor for the first time. The blank quartz plates with different thicknesses were set in the solution and their vibrations were excited and detected by the line antenna without contacting. One channel was covered by BSA, and its response was subtracted from the other channel responses as the reference. The exponential frequency change was observed in each channel, and its exponential coefficient was found to be useful for evaluating the binding reaction rather than the amount of the frequency change. The five channel biosensor was then applied to monitor the specific and nonspecific bind-

ing reactions simultaneously, and it demonstrated the successful operation as the multichannel immunosensor. This paper showed 10 channels for the simultaneous vibration measurement, but this is not the maximum number. Further increase of the channel number will require reducing the size of the quartz plate for setting all the crystals in the same environment.

Acknowledgement

This study was supported by Life Phenomena and Measurement Analysis, PRESTO, by Japan Science and Technology Agency.

References

(1) Muramatsu, H.; Dicks, M. D.; Tamiya, E.; Karube, I. Anal. Chem. 1987, 59, 2760-2763.

(2) Liu, Y.; Yu, X.; Zhao, R.; Shangguan, D.; Bo, Z.; Liu, G. Biosens. Bioelectron. 2003, 19, 9-19.

(3) Ogi, H.; Nagai, H,; Fukunishi, Y.; Hirao, M.; Nishiyama, M.; Anal. Chem. 2009, 81, 8068-8073.

(4) Pope, L. H.; Allen, S.; Davies, M. C.; Roberts, C. J.; Tendler, S. J. B.; Williams, P. M. Langmuir. 2001, 17, 8300-8304.

(5) Yang, A. Y.; Rawle, R. J.; Selassie, C. R. D.; Johal, M. S. Biomacromolecules, 2008, 9, 3416-3421.

(6) Baur, J.; Gondran, C.; Holzinger, M.; Defrancq, E.; Perrot, H.; Cosnier, S. Anal. Chem. in press. DOI: 10.1021/ac9024329.

(7) Cans, A. S.; Hook, F.; Shupliakov, O.; Ewing, A. G.; Eriksson, P. S.; Brodin, L.; Orwar, O. Anal. Chem. 2001, 73, 5805-5811.

(8) Kang, H. W,; Muramatsu, H. Biosens. Bioelectron. 2009, 24, 1318-1323.

(9) Pan, Y.; Guo, M.; Nie, Z.; Huang, Y.; Pan, C.: Zeng, K.; Zhang, Y.; Yao, S. Biosens. Bioelectron. in press. doi:10.1016/j.bios.2009.11.022.

(10) Eddowes, M. J. Biosensors. 1987, 3, 1-15.

(11) Ebara, Y.; Itakura, K.; Okahata, Y. Langmuir. 1996, 12, 5165-5170.

(12) Ogi, H.; Ohmori, T.; Hatanaka, K.; Hirao, M.; Nishiyama, M. Jpn. J. Appl. Phys. 2008, 47, 4021-4023.

(13) Wang, H,; Wang, J.; Choi, D.; Tang, Z.; Wu, H.; Lin, Y. Biosens. Bioelectron. 2009, 24, 2377-2383.

(14) Kim, D. M.; Noh, H. B.; Park, D. S.; Ryu, S. H.; Koo, J. S.; Shim, Y. B. Biosens. Bioelectron. 2009, 25, 456-462.

(15) Tatsuma, T.; Watanabe, Y.; Oyama, N. Anal. Chem. 1999, 71, 3632-3636.

(16) Dickert, F. L.; Lieberzeit, P. A.;Achatz, P.; Palfinger, C.; Fassnauer, M.; Schmid, E.; Werthera, W.; Hornerb, G. Analyst. 2004, 129, 432-437.

(17) Abe, T.; Esashi, M. Sens. Actuat. A. 2000, 82, 139-143.

(18) Hung, V. N.; Abe, T.; Minh, P. N.; Esashi, M. Appl. Phys. Lett. 2002, 81, 5069-5071.

(19) Hung, V. N.; Abe, T.; Minh, P. N.; Esashi, M. Sens. Actuat. A. 2003, 108, 91-96.

(20) Jin, X.; Huang, Y,; Mason, A.; Zeng, X. Anal. Chem. 2009, 81, 595-603.

(21) Zhang, B.; Mao, Q.; Zhang, X.; Jiang, T.; Chen, M.; Yu, F.; Fu, W. Biosens. Bioelectron. 2004, 19, 711-720.

(22) Ogi, H.; Motohisa, K.; Matsumoto, T.; Hatanaka, K.; Hirao, M. Anal. Chem. 2006. 78, 6903-6909.

(23) Ogi, H.; Motohisa, M.; Hatanaka, K.; Ohmori, T.; Hirao, M.; Nishiyama, M. Biosens. Bioelectron. 2007, 22, 3238-3242.

(24) Ogi, H.; Fukunishi, Y.; Omori, T.; Hatanaka, K.; Hirao, M.; Nishiyama, M. Anal. Chem. 2008, 80, 5494-5500.

(25) Ogi, H.; Fukunishi, Y.; Nagai, H.; Okamoto, K.; Hirao, M.; Nishiyama, M. Biosens. Bioelectron. 2009, 24, 3148-3152.

(26) Hirao, M., Ogi, H., Fukuoka, H. Rev. Sci. Instrum. 1993, 64, 3198-3205.

(27) Petersen, G. L. ; Chick B. B.; Fortunko, C. M.; Hirao, M. Rev. Sci. Instrum. 1994, 65, 192-198.

(28) Ogi, H.; Motohisa, K.; Hatanaka, K.; Ohmori, T.; Hirao, M.; Nishiyama, M. Jpn. J. Appl. Phys. 2007, 46, 4693-4697.

(29) Kronvall, G.; Quie, P. G. ;Williams, R. C. Jr. J. Immunol. 1970, 104, 273-278.

(30) Hanson, D. C. ; Schumaker, V. N. J. Immunol. 1984, 132, 1397-1409.

(31) Kessler, S. W. J. Immunol. 1975, 115, 1617-1624.

(32) Hanson, D. C. ; Phillips, M. L. ; Schumaker. V. N. J. Immunol. 1984, 132, 1386-1396.

Figure Caption

Fig. 1 Schematic of the multichannel sensor cell. The two antenna wires are embedded in the bottom Teflon block, and the thin grounding foil is in the top Teflon block. The silicon rubbers lightly grasp parts of edges of the quartz plates.

Fig. 2 Resonance spectrum from ten channel quartz plates with different thicknesses between 30 and 39 μm immersed in PBS measured by the line antenna wires contactlessly.

Fig. 3 (Color online)Schematics of five channel quartz surfaces.

Fig. 4 Frequency changes of the three channel WE-MQCM caused by the injection of a 515 nM hIgG solution (broken lines). The reference channel indicates the quartz plate covered by BSA through the SAM. The other two channels are SPA-immobilized quartz plates. The concentration values indicate the SPA concentrations in the immobilization process. The solid lines are frequency changes, where the reference channel response is subtracted.

Fig. 5 (Color online) Resonance frequency changes caused by the injection of (a) 50 nM hIgG, (b) 50 nM mIgG, and (c) 50 nM rIgG solutions. (d)-(e) are frequency changes of the four channels, where the response of the reference channel (BSA channel) is subtracted.

Fig. 6 Exponential coefficients in the frequency changes of various specific and nonspecific binding reactions.

References

.

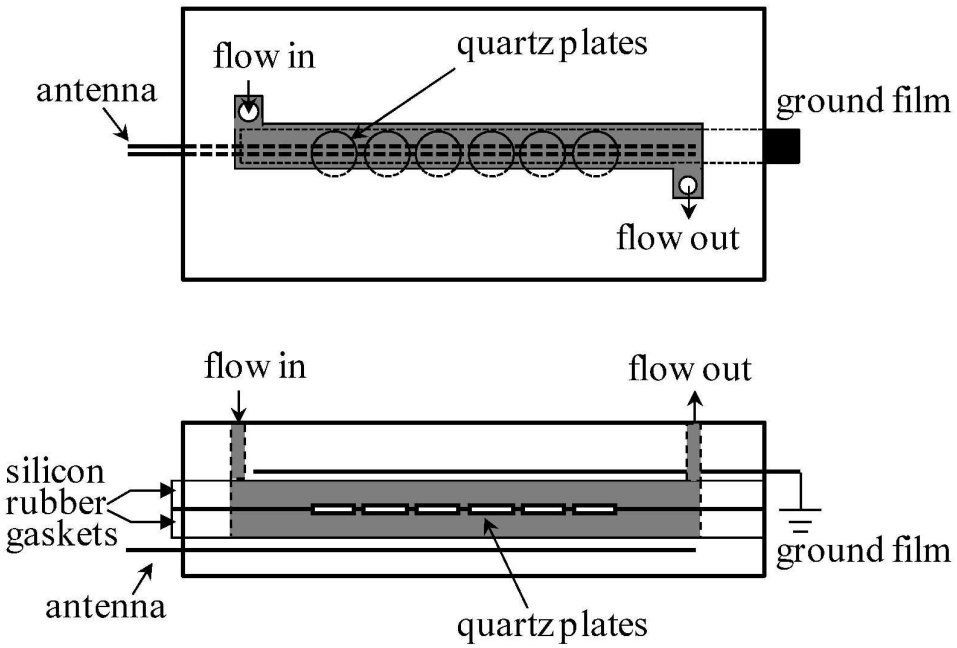

140x92mm (600 x 600 DPI)

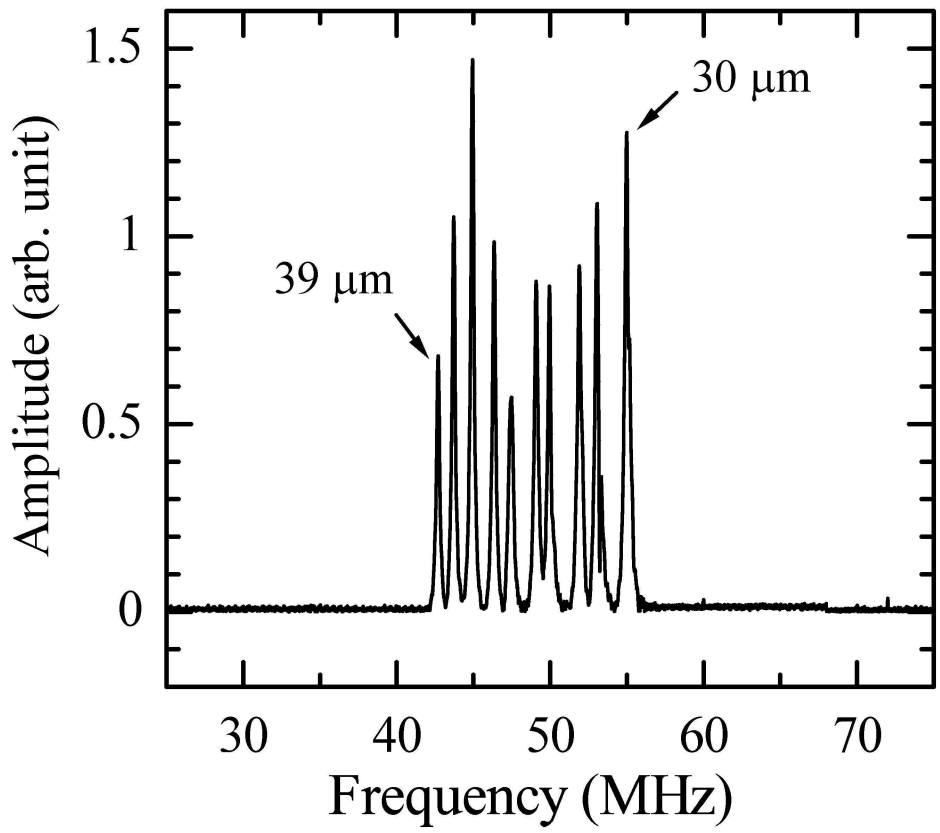

121x105mm (600 x 600 DPI)

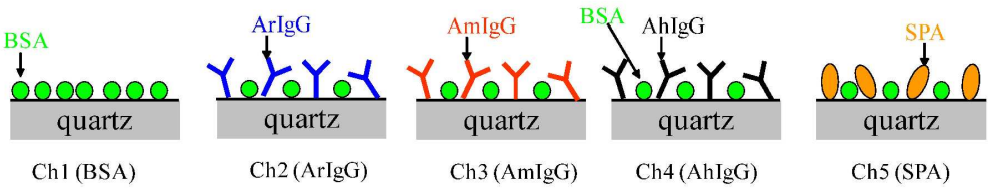

229x45mm (600 x 600 DPI)

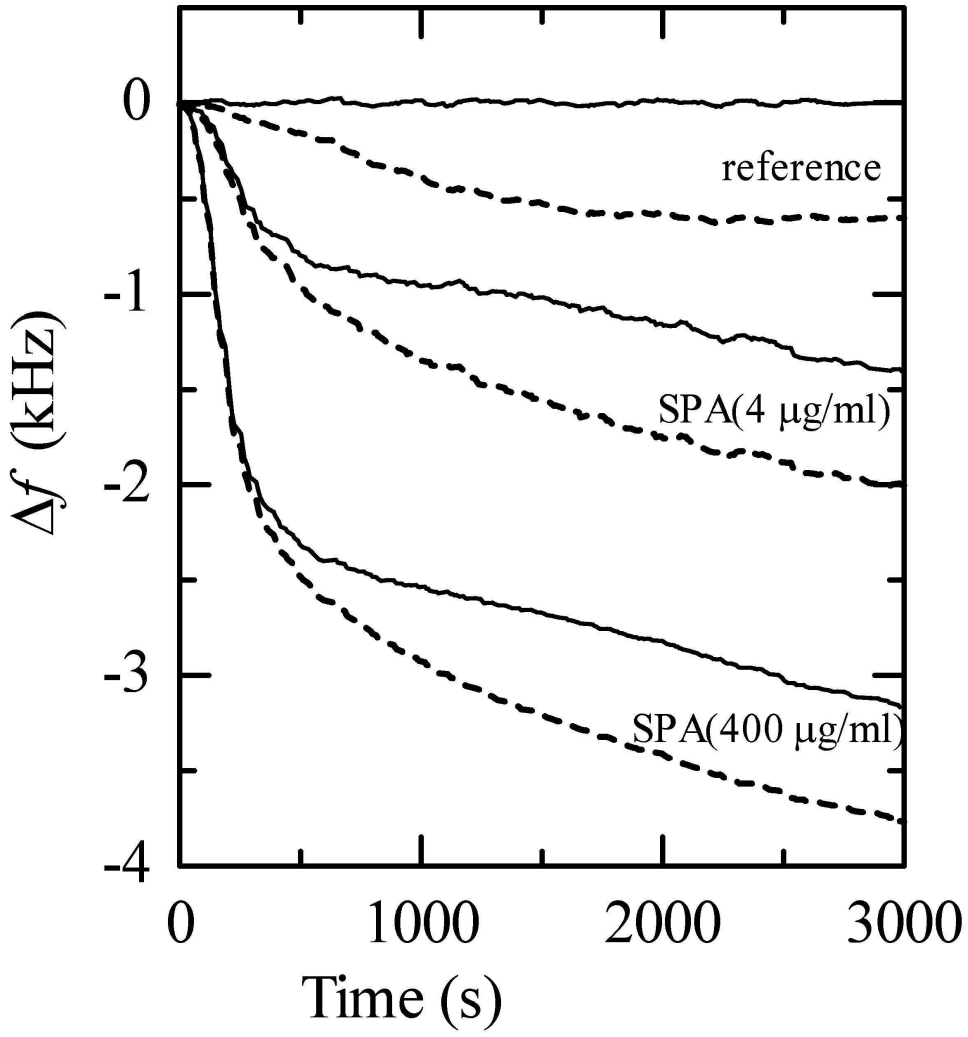

102x109mm (600 x 600 DPI)

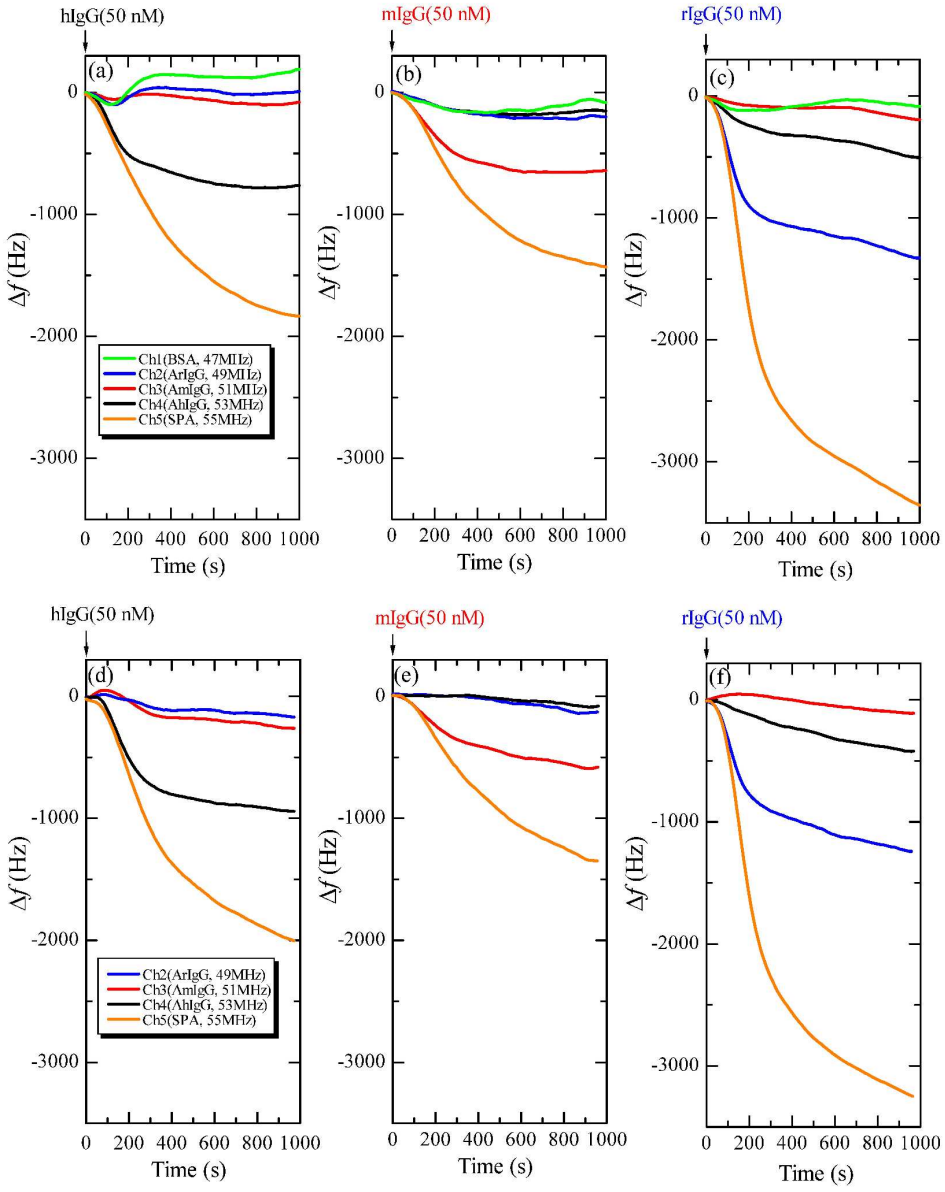

282x351mm (600 x 600 DPI)

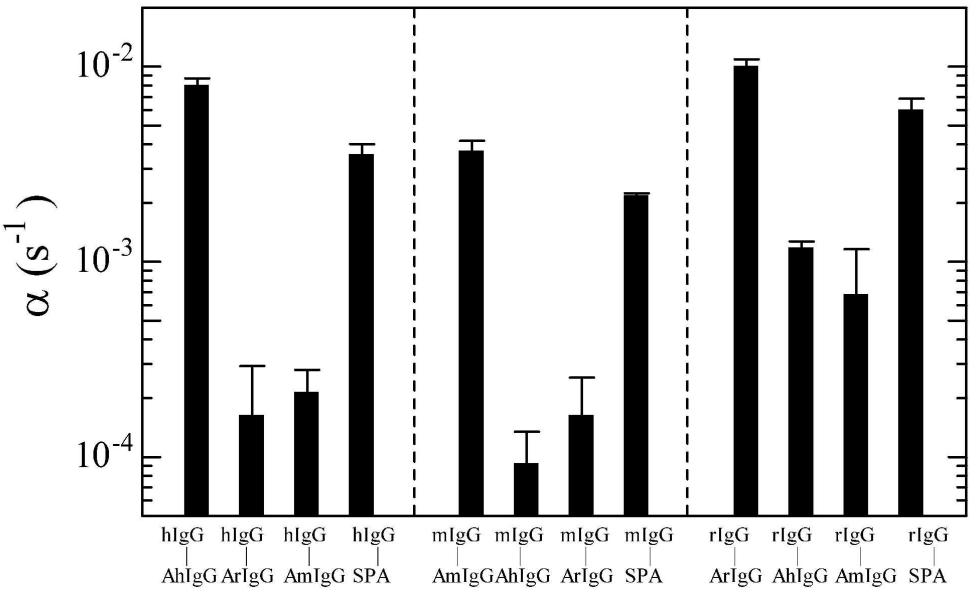

168x102mm (600 x 600 DPI)